AFRL-AFOSR-VA-TR-2018-0300

Laser Refrigeration of Optically-Insulated Cryophotonic Nanocrystals

Peter Pauzauskie
UNIVERSITY OF WASHINGTON

01/17/2018
Final Report

Air Force Research Laboratory
AF Office Of Scientific Research (AFOSR)/ RTA1
Arlington, Virginia 22203
Air Force Materiel Command

REPORT DOCUMENTATION PAGE

Form Approved
OMB No. 0704-0188

1. REPORT DATE *(DD-MM-YYYY)*	2. REPORT TYPE	3. DATES COVERED *(From - To)*
03-08-2018	Final Performance	15 Jul 2012 to 29 Dec 2015

4. TITLE AND SUBTITLE
Laser Refrigeration of Optically-Insulated Cryophotonic Nanocrystals

5a. CONTRACT NUMBER

5b. GRANT NUMBER
FA9550-12-1-0400

5c. PROGRAM ELEMENT NUMBER
61102F

6. AUTHOR(S)
Peter Pauzauskie

5d. PROJECT NUMBER

5e. TASK NUMBER

5f. WORK UNIT NUMBER

7. PERFORMING ORGANIZATION NAME(S) AND ADDRESS(ES)
UNIVERSITY OF WASHINGTON
4333 BROOKLYN AVE NE
SEATTLE, WA 98195-0001 US

8. PERFORMING ORGANIZATION REPORT NUMBER

9. SPONSORING/MONITORING AGENCY NAME(S) AND ADDRESS(ES)
AF Office of Scientific Research
875 N. Randolph St. Room 3112
Arlington, VA 22203

10. SPONSOR/MONITOR'S ACRONYM(S)
AFRL/AFOSR RTA1

11. SPONSOR/MONITOR'S REPORT NUMBER(S)
AFRL-AFOSR-VA-TR-2018-0300

12. DISTRIBUTION/AVAILABILITY STATEMENT
A DISTRIBUTION UNLIMITED: PB Public Release

13. SUPPLEMENTARY NOTES

14. ABSTRACT
The demonstration of anti-Stokes laser refrigeration to cryogenic temperatures with macroscopic YLF crystals doped with Yb3+ rare-earth ions has resulted in a new approach for solid state laser refrigeration. There are remarkable changes in a materials density of states (electron, phonon, or photon), optical absorption, radiative lifetime, thermal conductivity, and light scattering properties when the materials size is reduced below optical wavelengths. One outstanding question in the field is the extent to which a nanoscale YLF crystals size and morphology will enhance its external radiative quantum efficiency and subsequent performance in solid state laser refrigeration.

15. SUBJECT TERMS
sensor, adaptive

16. SECURITY CLASSIFICATION OF:			17. LIMITATION OF ABSTRACT	18. NUMBER OF PAGES	19a. NAME OF RESPONSIBLE PERSON
a. REPORT	b. ABSTRACT	c. THIS PAGE			POMRENKE, GERNOT
Unclassified	Unclassified	Unclassified	UU		19b. TELEPHONE NUMBER *(Include area code)* 703-696-8426

Standard Form 298 (Rev. 8/98)
Prescribed by ANSI Std. Z39.18

Final Performance Report to AFOSR
AFOSR contract FA9550-12-1-0400
Laser Refrigeration of Optically-Insulated Cryophotonic Nanocrystals
period: July 14, 2012- December 29th, 2015

PI: Prof. Peter Pauzauskie
Department of Materials Science & Engineering
University of Washington
302D Roberts Hall
Seattle, WA 98103
Tel. 206-543-2303
Email: peterpz@uw.edu

To: technicalreports@afosr.af.mil
Subject: Final Performance Report to Dr. Gernot Pomrenke

Contract/Grant Title: Laser Refrigeration of Optically-Insulated Cryophotonic Nanocrystals
Contract/Grant #: FA9550-12-1-0400
Reporting Period: 14 July 2012 to 29 December 2015

FINAL PERFORMANCE REPORT

1. **Executive summary**:

Laser refrigeration has been of interest to the wider scientific community for applications in cooling macroscopic components including thermal focal plane array detectors, reference cavities for sensitive laser interferometers, and more recently for the development of high-power radiation-balanced-lasers (RBLs). Nanoscale materials have a number of advantages relative to their bulk/Czochralski single-crystal counterparts in terms of scalable manufacturing and low-cost solution-phase processing. However, at the outset of this project it remained an outstanding question whether nanoscale materials could undergo laser refrigeration in condensed/liquid media such as liquid water. The research funded by this grant produced the first experimental demonstration of "cold Brownian motion" / laser refrigeration in a condensed phase [Roder et al., PNAS, 2015] through the development of unique single-beam laser-trapping/cooling instrumentation. The research results presented by the Pauzauskie laboratory in the scientific literature has changed the scientific community's thinking about how laser refrigeration materials can be used at nanometer length scales, including a large number of potential applications of nanoscale laser refrigeration crystals. For instance, nanocrystalline materials could serve as an active cooling agent in composite oxide/fluoride fiber/cladding designs under consideration for future radiation balanced lasers. In the quantum physics community this research has inspired the use of laser refrigeration materials are being considered for reaching quantum mechanical ground states of nano- to micron-scale crystals [https://arxiv.org/abs/1703.07155] or for the laser refrigeration of optical NV-point-defects/qubits in diamond [https://arxiv.org/abs/1701.08505].

2. Objectives:

There were three primary research objectives for this project. The first objective was to develop low-cost hydrothermal processing methods to produce Yb(III):$YLiF_4$ laser-refrigeration ceramics for applications in solid state laser refrigeration. The current state of the art for these materials is bulk Czochralski single-crystal growth this is expensive, slow (week to month time scales), and hazardous in that it involves gas-phase HF.

The second objective was to develop single-particle laser-trapping/thermometry methods in both liquid water and vacuum environments to investigate the fundamental cooling limits of YLF materials. Experiments using laser trapping in liquid environments were designed to establish whether solid state laser refrigeration could be used to observe laser cooling in condensed phases, including liquid water, for the first time. Vacuum trapping experiments were motivated by establishing the minimum achievable temperatures for laser cooling in a vacuum environment, free from heat sources that arise from physical contact.

The third objective was to develop predictive, closed-form mathematical heat-transfer models for applications in characterizing solid-state laser-refrigeration / heat-transport phenomena add nanometers length scales. These models are useful for calibrating and interpreting experimental measurements of laser heating and cooling in an optical trap.

2.1. Cumulative lists of people involved in the research effort:

Dr. Paden B. Roder (UW, MSE PhD student); currently an engineer at Intel
Dissertation: "*Temperature Extraction of Engineered Nanoparticles in an Optical Trap*"

Dr. Bennett E. Smith (UW, Physical Chemistry PhD student); currently an engineer at Intel
Dissertation: "*Thermochemical Dynamics of Laser-Irradiated Semiconductor Nanostructures*"

Xuezhe Zhou (UW, MSE PhD student); currently an engineer at Apple

Emeritus Prof. E. James Davis (UW, ChE)

Assistant Prof. Peter J. Pauzauskie (UW, MSE); recently promoted to Associate Professor

2.2. Publications stemming from the research effort:

1.) Smith, B.E.; Zhou, X.; Davis, E.J.; Pauzauskie, P.J.; "Photothermal heating of nanoribbons." Optical Engineering (2017) 56:011111.

2.) Zhou, X.; Roder, P.B.; Smith, B.E.; Pauzauskie, P.J.; "Laser refrigeration of rare-earth doped sodium-yttrium-fluoride nanowires." Proc. SPIE 10121, Optical and Electronic Cooling of Solids II, 1012103 (Feb 17, 2017).

3.) Roder, P.B.; Manandhar, S.; Devaraj, A.; Perea, D.E.; Davis, E.J.; Pauzauskie, P.J.*; "Pulsed photothermal heating of one-dimensional nanostructures." Journal of Physical Chemistry C, 120(38), 21730-21739, (2016).

4.) Zhou, X.; Smith, B.E.; Roder, P.B.; Pauzauskie, P.J.*; "Laser refrigeration of ytterbium-doped sodium yttrium fluoride nanocrystals." Advanced Materials, 28(39), 8658-8662, (2016).

5.) Smith, B.E.; Zhou, X.; Roder, P.B.; Abramson, E.H.; Pauzauskie, P.J.*; "Recovery of hexagonal Si-IV nanowires from extreme GPa pressure." Journal of Applied Physics, 119(18), 185902, (2016).

6.) Roder, P.B.; Smith, B.E.; Zhou, X.; Crane, M.J.; Pauzauskie, P.J.*; " Laser Refrigeration of hydrothermal nanocrystals in physiological media." Proceedings of the National Academy of Sciences, 112(49), 15024-15029, (2015).

7.) Smith, B.E.; Roder, P.B.; Zhou, X.; Pauzauskie, P.J.*; "Hot Brownian thermometry and cavity-enhanced harmonic generation with nonlinear optical nanowires." Chemical Physics Letters, 639, 310-314, (2015). (invited cover feature)

8.) Roder, P.B.; Smith, B.E.; Davis, E.J.; Pauzauskie, P.J.*; "Photothermal superheating of water with ion-implanted silicon nanowires." Advanced Optical Materials, 3, 1362-1367, (2015).

9.) Crane, M.J.; Pauzauskie, P.J.*; "Mass transport in nanowire synthesis: an overview of scalable nanomanufacturing.", Journal of Materials Science & Technology, 31 523-532 (2015), [invited article].

10.) Smith, B.E.; Roder, P.B.; Zhou, X.; Pauzauskie, P.J.*; "Singlet oxygen generation from individual semiconducting and metallic nanostructures during near-infrared laser trapping.", ACS Photonics, 2 559-564 (2015).

11.) Smith, B.E.; Roder, P.B.; Zhou, X.; Pauzauskie, P.J.*; "Nanoscale materials for hyperthermal theranostics." Nanoscale, 7, 7115-7126, (2015), [invited review article].

12.) Manandhar, S.; Roder, P.B.; Hanson, J.; Wilbur, D.S.W.; Pauzauskie, P.J.*; "Rapid sol-gel synthesis of nanodiamond aerogel.", Journal of Materials Research, 29 2905-2911 (2014), [invited].

13.) Roder, P.B.; Smith, B.E.; Davis, E.J.; Pauzauskie, P.J.*; "Photothermal Heating of Nanowires." J. Phys. Chem. C, 118, 1407 – 1416, (2014).

14.) Roder, P.B.; Pauzauskie, P.J.*; Davis, E.J.; "Nanowire Heating by Optical Electromagnetic Irradiation." Langmuir 28 16177 – 16185 (2012).

3. Accomplishments

a. ***The first experimental demonstration of cold Brownian motion***.

Single-beam laser tweezers were used for the first time to simultaneously optically-trap and laser-refrigerate single nano- and micro-crystals of yttrium-lithium-fluoride ($YLiF_4$) ceramic materials that were substitutionally doped with 10% Yb(III) ions. The ceramic grains were trapped in aqueous electrolyte solutions, and were observed to lower the temperature of D2O by more than 20°C starting from room temperature. This led to the first experimental demonstration of "cold Brownian motion" since Einstein's seminal paper on equilibrium Brownian motion published in 1905.

b. L*aser refrigeration of hexagonal (β) phase NaYF4*.

Hexagonal NaYF4 materials have been theoretically predicted to be excellent materials for solid state laser refrigeration. However, the literature contains to experimental laser refrigeration efforts because it cannot be growth with conventional Czochralski single-crystal methods to unavoidable material cracking from anisotropic thermal expansion coefficients. We used a novel hydrothermal approach to grow nanowires of this material and showed for the first time that individual β-NaYF4 NWs doped with Yb(III) ions can be optically trapped and refrigerated by an NIR, continuous-wave laser source in a fluid medium. These results show the potential of using β-NaYF4: 10%Yb3+ NWs for applications in localized optoelectronic device cooling and physiological laser refrigeration.

c. ***Predictive analytical solutions for heat transfer equation for laser-irradiated nanostructures***.

Analytical mathematical models were derived to help quantify heat transfer during single beam laser trapping experiments. The mathematical model of photothermal heating was extended to quantify the kinetics of heat transfer for semiconductor (cadmium sulfide, CdS) nanoribbon structures that were reported to cool under visible laser irradiation in a 2013 Nature paper. Experiments also were performed to evaluate how well theoretical models dpredicted laser heating in single-beam laser trapping experiments. During these experiments we observed potential chemical reactions at the

semiconductor/liquid interface. To better understand these phenomena we performed laser trapping experiments using a sensing molecule, singlet-oxygen-senor-green (SOSG) to evaluate whether single-oxygen molecules may be produced during laser trapping experiments. We were able to confirm for the first time that singlet oxygen molecules can be produced from optically trapped semiconductor and metallic nanostructures.

d. ***Observation of Mie resonances for sum frequency generation in potassium niobate nanowires***.

The theoretical heat transfer model we developed predicted that laser heating would be maximized in semiconductor nanowires with diameters that matched classical Mie resonances. These results led to an invited feature paper at the Journal of Chemical Physics. Based on this invitation, we pursued experiments with nonlinear-optical nanowires to investigate morphology dependent cavity resonances could enhance second-harmonic generation and sum-frequency generation optically trapped nanowires. Our results demonstrated that Mie resonances are observable for both SHG and SFG processing in optically-trapped nanostructures, suggesting potential applications in enhancing the absorption of materials designed for solid-state laser refrigeration applications.

4. Optical trapping in liquids and the first experimental demonstration of "cold Brownian motion".

Our experimental research efforts demonstrated that low-cost, hydrothermal materials can be used in place of expensive, slow single-crystal Czochralski materials for manufacturing high-quality laser-refrigeration materials. Recently developed theory for "hot Brownain motion" was used to interpret experimental measurements of both photothermal heating and also the first experimental report of 'cold Brownian motion' in a condensed/liquid phase since Einstein's seminal 1905 paper on Brownian motion at thermodynamic equilibrium.

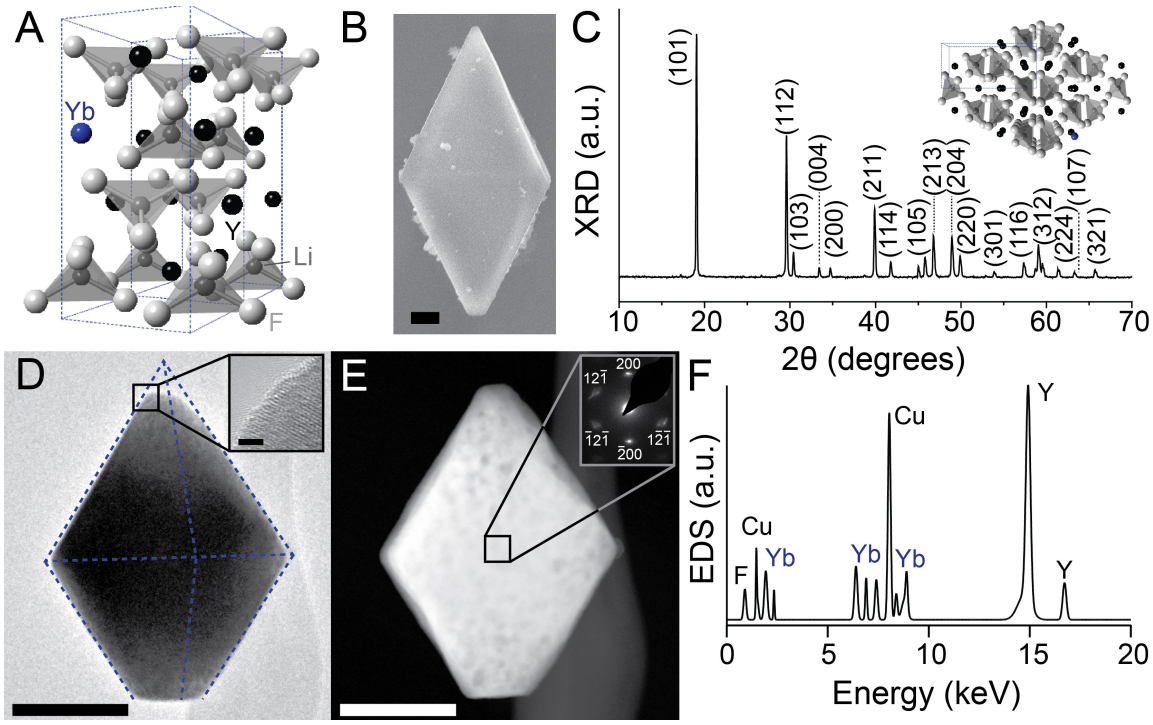

Fig. 1. Synthesis and characterization of YLF crystals. (A) Schematic of Scheelite crystal structure of YLF with I41/a space group symmetry. (B) Scanning electron microscope image of a faceted $Yb^{3+}_{0.1}Y^{3+}_{0.9}LiF_4$ particle exhibiting TTB morphology. Scale bar = 1 μm. (C) Powder x-ray diffraction pattern of YLF crystals following hydrothermal synthesis indicating a pure Scheelite crystal phase. Inset: schematic of TTB morphology relative to YLF's unit cell. (D) Bright field transmission electron microscope (TEM) image of an individual Yb^{3+}:YLF grain; scale bar = 200 nm. Inset: high-resolution TEM image taken from the indicated region; scale bar = 2 nm. (E) High-angle annular-dark-field (HAADF) image of the YLF grain in panel B showing regions of high contrast suggesting the presence of polycrystalline domains. Inset: select area electron diffraction from the indicated region. (F) X-ray fluorescence compositional-analysis-spectrum of an individual YLF crystal taken within the TEM confirming the elemental crystalline composition including Y, Yb, and F species.

The temperature of single nanoscale ceramic particles was quantified during single-beam laser trapping experiments through analysis of the particle's Brownian dynamics / diffusion-coefficient as well as a Boltzmann analysis of emission from erbium (III) rare-earth ions co-doped within in the crystal lattice. Forward-scatter laser radiation was collected from an optically-trapped particles and dispersed on a quadrant photodiode. The photodiode signal was processed to retrieve the power-spectral-density for a given particle's motion. For the vast majority of dielectric materials and increase in the power of the trapping laser is observed to increase the temperature of the trapped particle. Experiments with Yb:YLF materials showed for the first time that increasing the optical power of the trapping laser

produced a decrease in the thermal Brownian motion of the trapped object shown below in Figure 2.

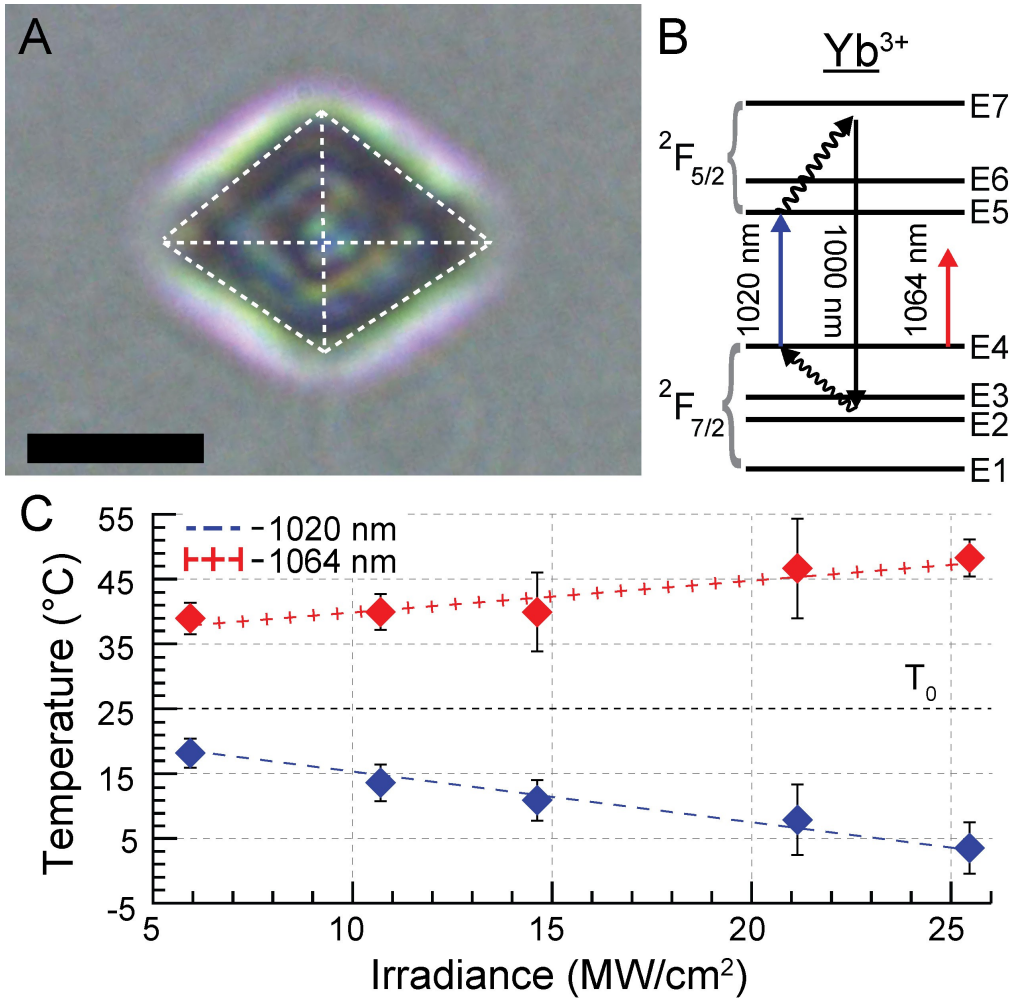

Fig. 2. Laser refrigeration of optically trapped YLF microcrystals. (A) Optical micrograph of an optically trapped YLF crystal; scale bar = 3 μm. (B) Crystal field energy level configuration of Yb^{3+} dopant ions and employed cooling scheme. (C) Extracted temperature of optically trapped particles in D_2O as determined using the outlined CBM analysis. Yb^{3+}-doped YLF particles are shown to cool when trapping wavelength is resonant with the E4-E5 transition (λ = 1020 nm) but heat when the trapping wavelength is below the transition (λ = 1064 nm).

If the trapping laser is detuned from the cooling resonance to lower energies, then a transition from cooling to heating is observed. Experimentally, this was performed using a Nd:YAG laser at a wavelength of 1064 nm instead of a laser trap at 1020 nm. These results represent the first experimental demonstration of cold Brownian motion since Einstein's seminar paper on Brownain motion at thermal equilibrium published in 1905.

5. First experimental demonstration of laser-refrigeration of $NaYF_4$.

Sodium–yttrium–fluoride (NaYF4) upconverting nanocrystals are currently being investigated for a range of applications including bioimaging, color displays, solar cells, and photocatalysis. Hexagonal β-NaYF4 has also been predicted to be a promising host for laser cooling; however, to date, the laser refrigeration of β-NaYF4 single crystals has not been reported due to challenges in bulk Czochralski crystal growth. We used a novel hydrothermal synthesis approach to synthesize nanowires of this material that exhibited hexagonal-prism morphology shown in Figure 3 below.

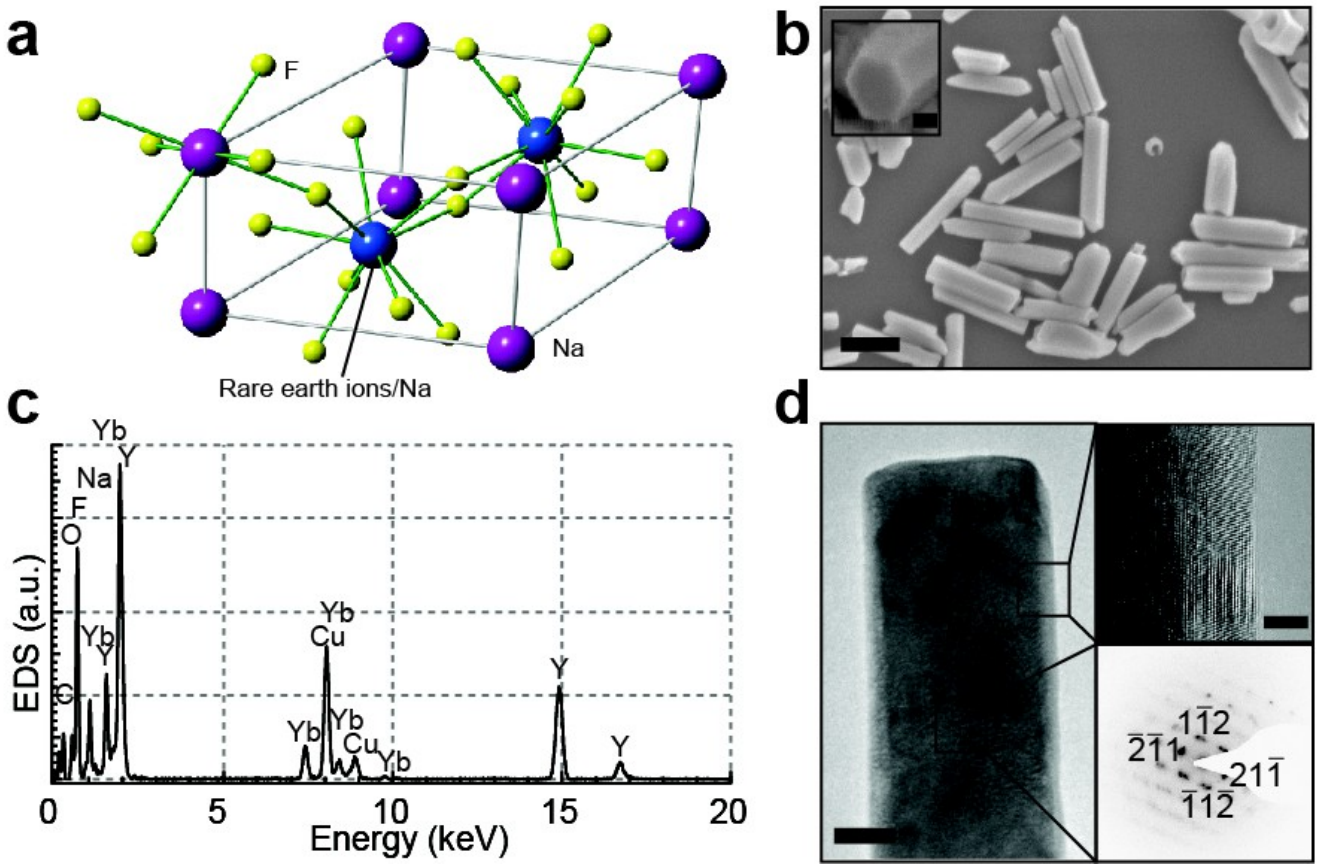

Fig. 3. Synthesis and characterization of $NaYF_4$ nanowires. (a) Schematic of hexagonal crystal structure of β-NaYF4 with P63/m space group symmetry. (b) SEM image of β-$NaYF_4$: 10%Yb^{3+} nanowires, scale bar = 500 nm. Inset: SEM image of a β-NaYF4:10%Yb^{3+} nanowire exhibiting an (001) end facet; scale bar = 100 nm. (c) X-ray fluorescence compositional-analysis-spectrum of an individual β-$NaYF_4$: 10%Yb^{3+} nanowire taken within the TEM confirming the elemental crystalline composition including Y, Yb, and F. (d) Bright field TEM image of β-$NaYF_4$: 10%Yb^{3+} nanowire; scale bar = 25 nm. Top inset: high-resolution TEM image taken from the indicated region; scale bar = 4 nm. Bottom inset: select area electron diffraction from the indicated region.

Single-beam laser trapping experiments were used to demonstrate that it is possible to refrigerate this

phase of $NaYF_4$ nanowires. Figure 4 below shows a crystal field diagram for Yb(III) ions within the NaYF4 nanowire materials.

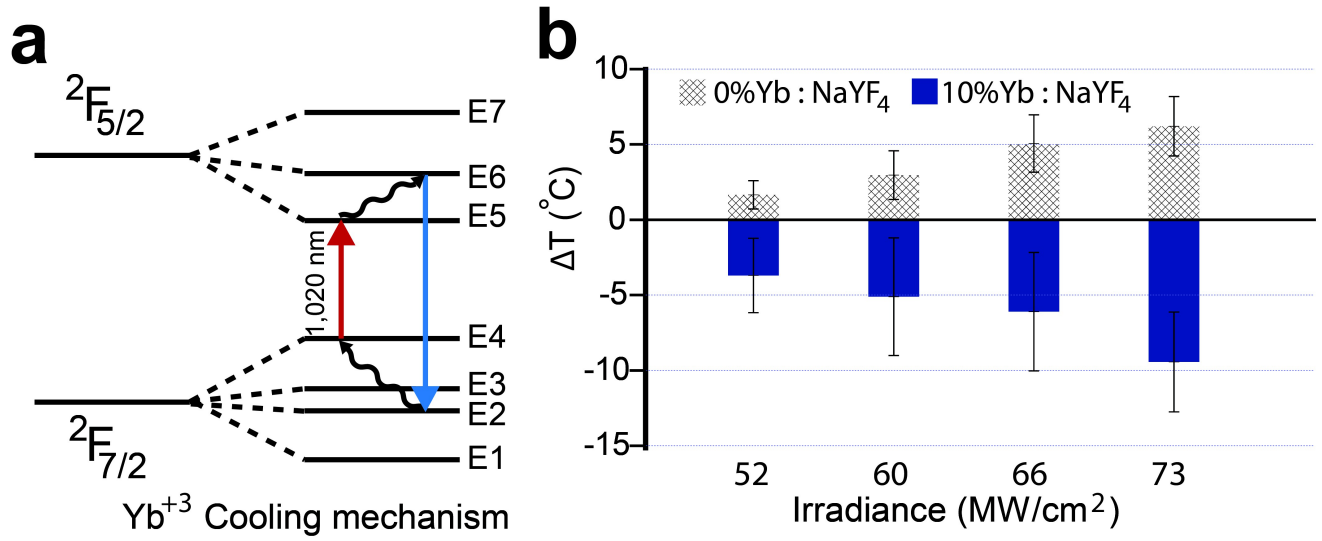

Fig. 4. (a) Diagram of the anti-Stokes laser refrigeration process. (b) Temperature change of individually trapped β-NaYF4 nanowires with different Yb^{3+} dopant concentrations under increasing 1020 nm laser irradiance. Error bars are based on standard deviation of 10 samples.

Cooling was observed in nanowire samples that were doped with 10%Yb(III) ions. Cooling was not observed in pure $NaYF_4$ nanowire materials that were not doped with Yb(III) ions, as shown above in Figure 4b.

6. Predictive analytical solutions for heat transfer equation for laser-irradiated nanostructures.

In order to gain confidence in laser cooling experiments we undertook efforts to build and test predictive, quantitative models of photothermal laser heating related to single-beam laser trapping. The models were based on classical product solutions of the heat conduction equation elaborated on in the references numbered 13 and 14 above in section 2.2 of this report. Numerical calculations were performed for cylindrical silicon nanowire cavities using both an infinite cylinder and also a finite cylinder as model geometries. Calculations with the infinite cylinder were pursued first because of well-known analytical solutions for Mie scattering from infinite cylinders. Although a measurable (>10 °C) amount of photothermal laser-heating of silicon nanowires is expected at large (MW/cm^2) laser-trapping irradiances, theoretical heat-transfer model predicted that the high thermal conductivity

of silicon would lead to minimal thermal gradients within individual nanowires. Calculations shown in Figure 5 below predicted that there would be a temperature variation on the order of 1 part in 10^6, even in scenarios where complex electric field profiles were established within the nanowires.

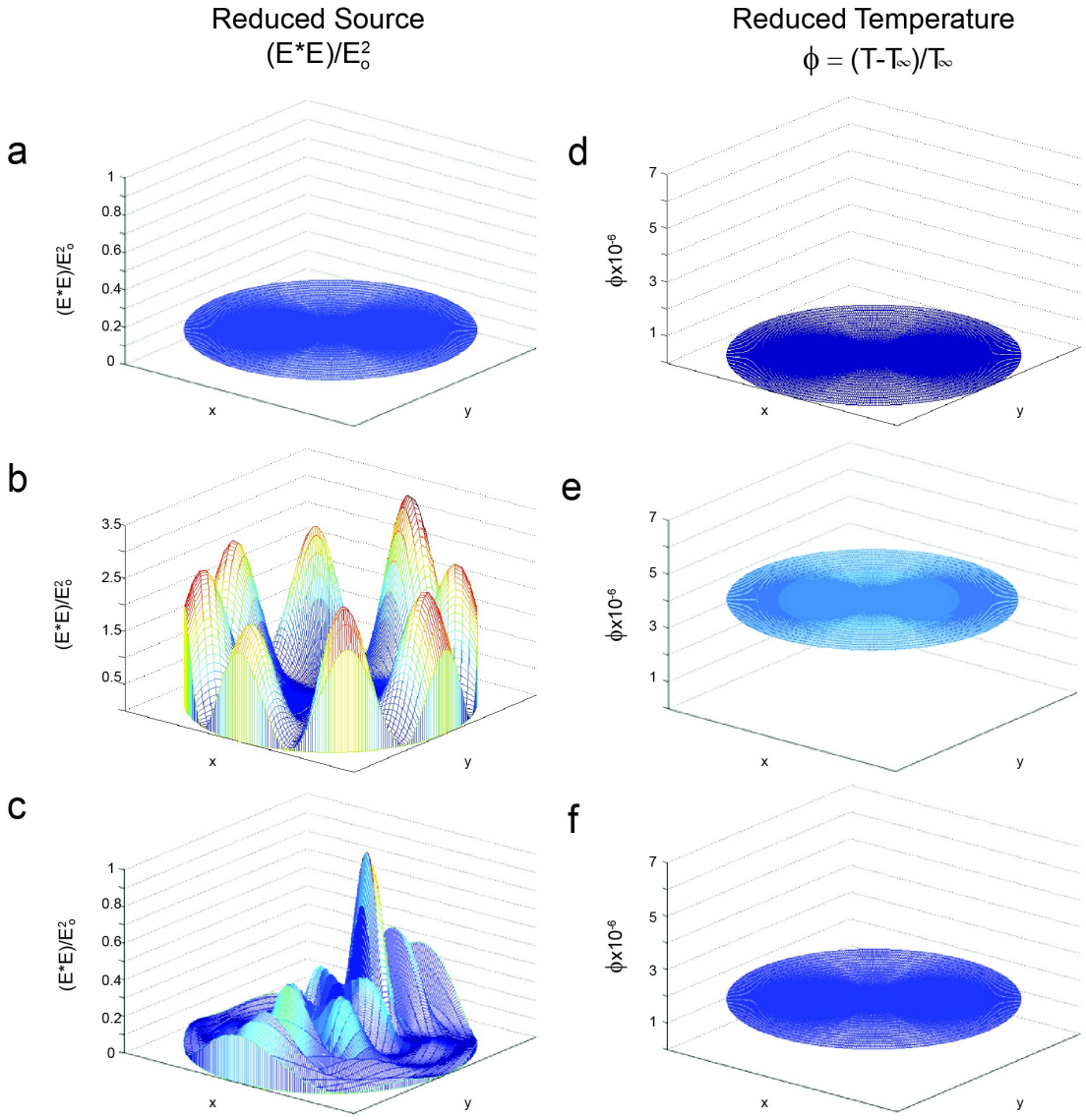

Fig. 5. Plots of the calculated normalized cross-sectional electromagnetic heating source term (a-c) and corresponding reduced cross-sectional temperature $\phi = (T-T_\infty)/T_\infty$ (d-f) for silicon nanowires in water with an outer diameter of 10 nm (a & d), 536 nm (b & e), and 1μm diameter(c & f) irradiated at $I_{inc} = 10^3$ W/cm^2 with a free-space wavelength of $\lambda = 980$ nm.

One important prediction of the classical product solution was the existence of morphology dependent resonances at nanowire diameters that led to the formation of electromagnetic whispering gallery modes (Fig. 5b) or standing waves (Fig. 5c) within the nanowire cavity. The observation of morphology dependent resonances was observed to be crucial for understanding the pulsed

photothermal heating of tapered nanowire structures commonly used in laser-assisted atom-probe-tomography characterization (Ref. 3 in the publications section).

7. Observation of Mie resonances in nanowire SHG and SFG.

The observation of morphology dependent cavity resonances in the laser heating of semiconductor nanowires led us to consider whether Fabry-Perot resonances may be observed in nonlinear SHG or SFG processes that occur in optically-trapped nanowire cavities. We pursued experiments with potassium niobate ($KNbO_3$) nanowires (KNNWs) shown below in Figure 6 using a continuous wave optical trapping laser that is tunable between 1020 and 1040 nm.

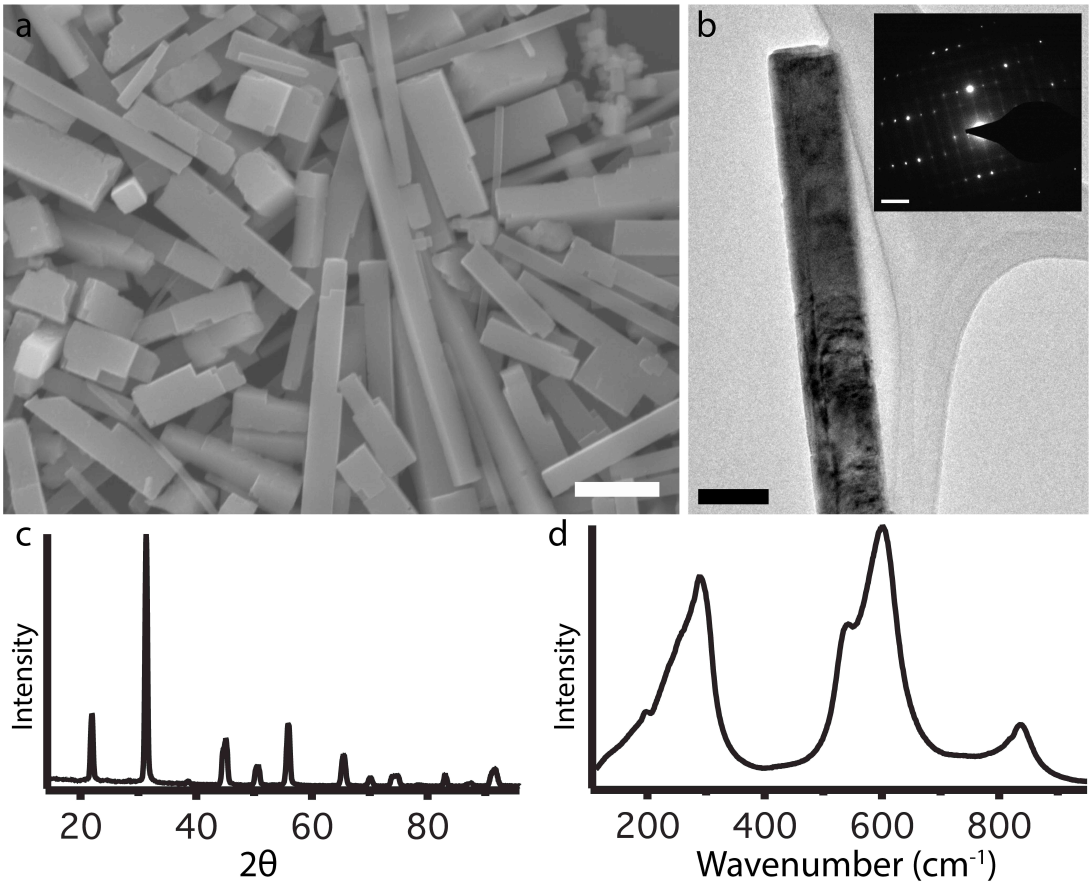

Fig. 6. Characterization of hydrothermally grown nanowires. a) Scanning electron micrograph of KNNWs demonstrating square cross-sections. Scalebar = 500 nm. b) Transmission electron micrograph of a single KNNW. Scalebar = 300 nm. c) Higher magnification of KNNW in b to show extended planar defects in a KNNW. Scalebar = 30 nm. d) Select area electron diffraction pattern of the KNNW in b. Scalebar = 5 nm^{-1} e) X-ray diffraction of a $KNbO_3$ powder sample with crystal planes indicated. Asterisk denotes peaks not associated with $KNbO_3$ and are likely from Nb metal precursor. f) Raman scattering from a $KNbO_3$ powder sample.

SHG was observed to be tunable based on the center wavelength of the trapping laser. Oscillations in the intensity of SHG signal were observed to be produced from the nanowire cavity while keeping the power of the optical trapping laser constant as shown below in Figure 7.

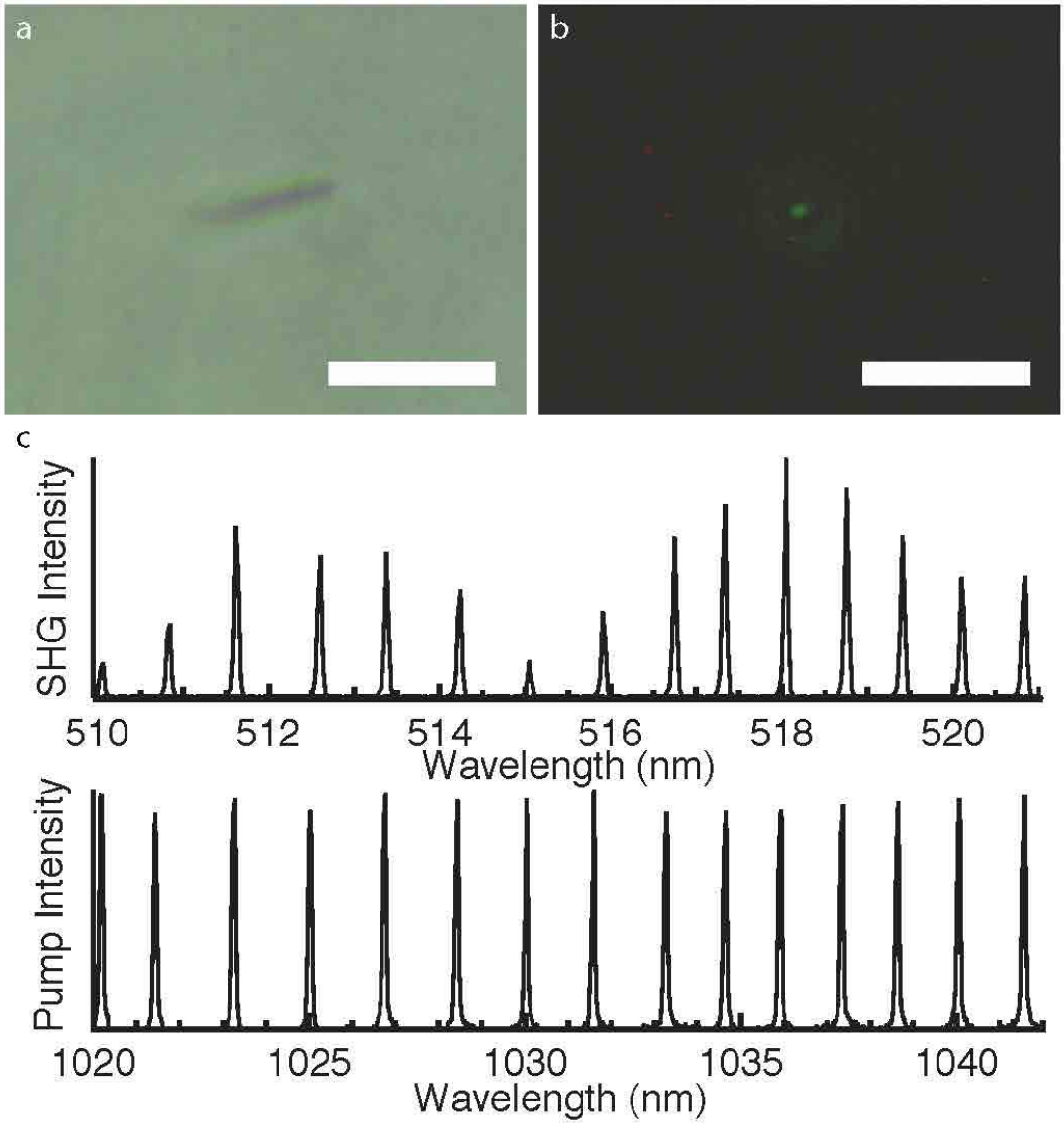

Fig. 7. (a) Bright field image of a KNNW in Brownian motion. Scale bar = 2 μm. (b) Long-exposure, dark image demonstrating SHG from the KNNW while trapped with a 1030 nm source. Scale bar = 2 μm. (c) A NIR tunable laser was tuned from 1020 to 1040 nm while maintaining a constant trapping power (lower panel). The second harmonic generation from a KNNW was detected at each discrete pump wavelength (upper panel). The oscillations with the SHG are interpreted to arise from Fabry-Perot resonances within the NW.

In addition to observing SHG, we were also able to observe SFG from optically trapped KNNWs. The fundamental 1064 nm lasing transition of a CW Nd:YAG laser was colinearly aligned with with tunable

trapping laser. When two different lasers were used to trap a single KNNW it was possible to observe SHG signal from each NIR laser, but also a new sum frequency signal that could be tuned in tandem with the tunable NIR laser as shown below in Figure 8.

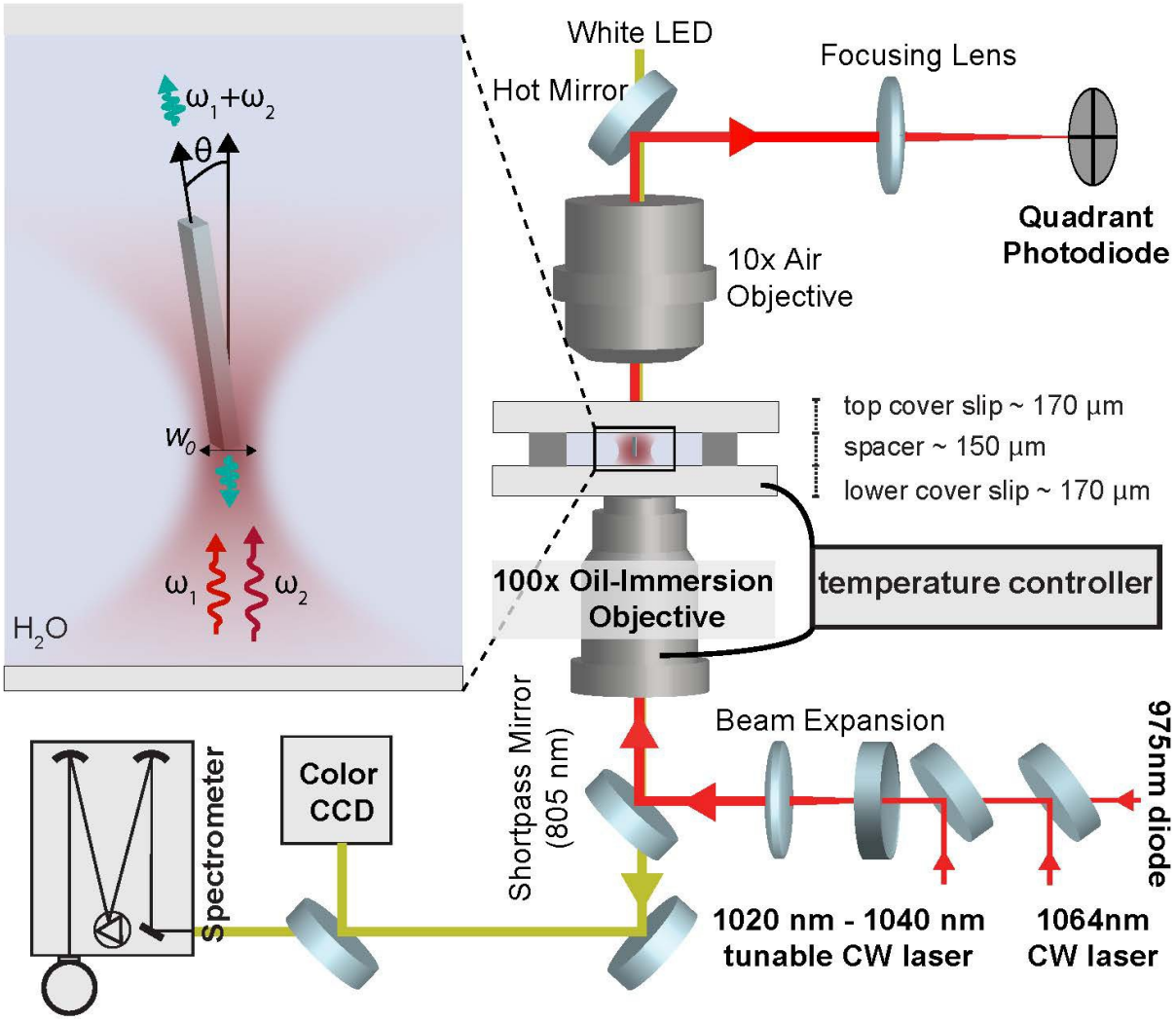

Fig. 8. Sum frequency generation from a KNNW using co-aligned lasers. Tunable sum frequency generation from a KNNW is possible using a co-aligned 1064 nm DPSS laser and a tunable 1020-1040 nm DPSS laser.

The observation of morphology dependent Mie resonances and Fabry-Perot resonances in subwavlength dielectric cavities suggests the potential for enhancing nanoscale solid-state laser refrigeration through designing laser-cooling materials with sizes that enhance photon confinement and the optical pumping wavelength of 1020 nm, but that are not resonant at blue-shifted wavelengths below 1020 nm.

9. **Conclusions & Future Work**

The most significant advance in this project was demonstrating that individual rare-earth doped nanocrystals can refrigerate their surrounding environment using single-beam laser-trapping experiments. This advance represents the first experimental demonstration of 'cold Brownian motion' since Einstein's seminar paper on Brownian motion in 1905. The figure below depicts the temperature field around a single laser-cooled nanocrystal in a fluid environment.

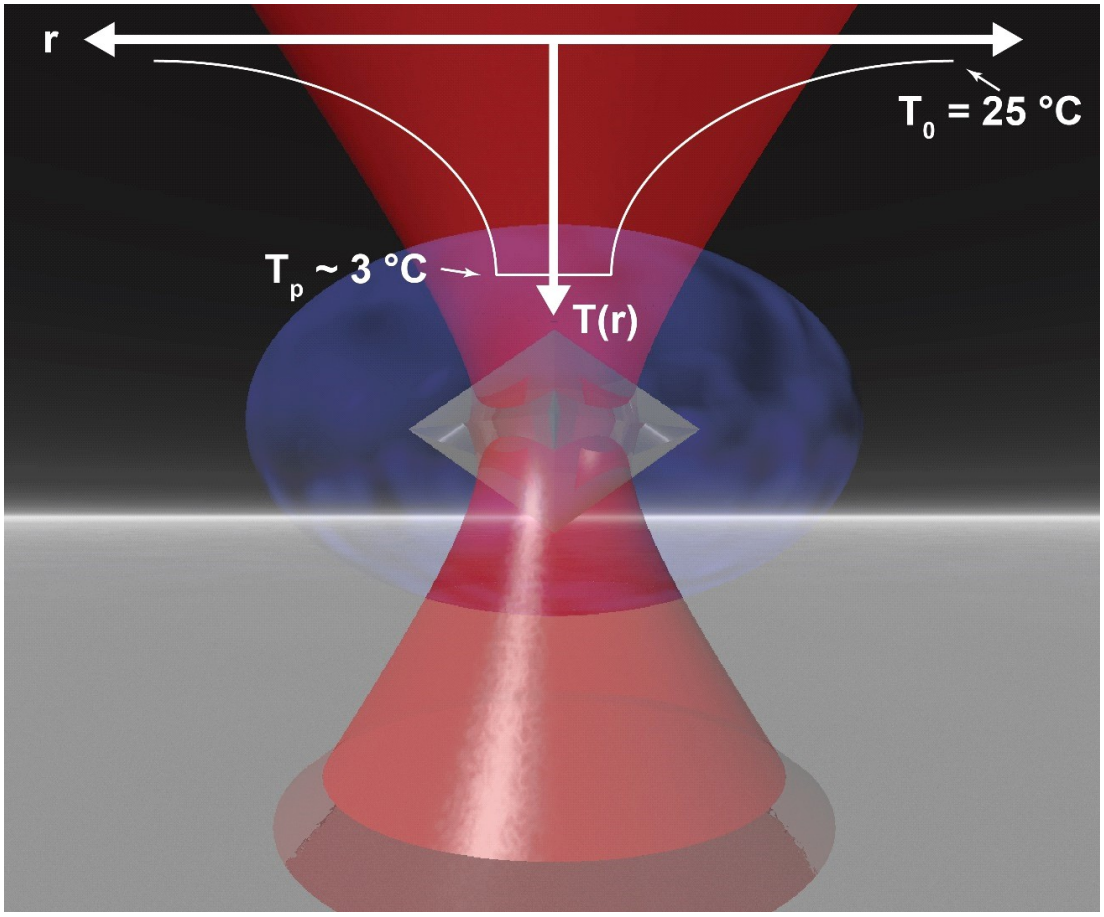

Fig. 9. Schematic of the first experimental observation of "cold Brownian motion." In this experiment, an incident laser simultaneously traps and refrigerates a dielectric particle within a fluid environment such that the temperature of both the particle and the fluid surrounding it are lowered below the ambient thermal temperature.

Measurements indicate that a particle refrigerates by approximately 20°C relative to the surrounding bath temperature. Calculations suggest that the fluid warms to within 95% of the ambient

temperature within approximately 7 particle diameters (7 micrometers) with the rise being inversely proportional to the distance from the particle's surface.

Unfortunately, unexpected challenges with suspending particle's in vacuum were compounded by unanticipated laser equipment failure during the course of this award, and it was not possible to pursue laser cooling experiments in vacuum. Since the end of this award in December 2015 two separate research labs in the “levitated optomechanics” / vacuum-trapping community have taken inspiration from our PNAS paper (publication #6 in section 2.2) and expressed interest in collaborating towards demonstrating ultra-cold trapped dielectric particles in vacuum. The first of these labs is led by Prof. Nick Vamivakas in the Physics department at U. Rochester, and the second lab is led by Prof. Peter Barker in the physics department at University College London. I am extremely interested in continuing to pursue laser refrigeration of cryophotonic materials in vacuum given many fascinating basic research applications including cooling the harmonic motion of macroscopic objects to their quantum mechanical ground state, experimental tests of quantum gravity, and active cooling of quantum information sources including the silicon and nitrogen vacancy centers in diamond.

We also are collaborating actively with colleagues in the integrated nanophotonics community [Arka Majumdar, UW-EE/Physics] to develop subwavelength laser refrigeration materials for us in active local cooling of optical heat sources within compact integrated photonic devices. Currently the only method available to mitigate heating in integrated photonic devices is to heat the entire photonic chip to an elevated temperature in order to reduce the relative heating induced from large laser powers passing through integrated waveguides, modulators, de-multiplexers, etc.. Chip-scale heating consumes a large fraction of the overall energy budget of an integrated photonic device. Laser refrigeration materials may be able to reduce this costly expenditure of resistive heating energy, and improve the energy efficiency / scalability of future integrated photonic circuits/devices.

In terms of the biological science community, the Pauzauskie laboratory has recently been contacted by several investigators interested in employing nanoscale laser cooling materials in the

study of the biochemical thermodynamics of single molecules [Prof. Iddo Heller @ VU-Netherlands], temperature/pressure sensing ion channels [Prof. Fred Sachs @ SUNY-Buffalo], and also the thermal control of enzymatic turn over frequencies [Prof. Joanna Aizenberg @ Harvard].

In terms of my current support for laser cooling research, I am a co-PI on a MURI award with a focus on the development of actively cooled radiation balanced lasers. More recently, my lab has helped with and is participating in a NSF-MRSEC grant (>$15M) with a partial focus on developing nanoscale laser refrigeration materials for use as the active element in future generations of cryogenic transmission electron microscopes.

Lastly, I conclude this report with the observation that this YIP award has made a profound contribution to helping launch my career at the University of Washington and I am most grateful to the AFOSR for this invaluable source of research support. In particular, I would like to thank (on behalf of myself and my graduate students) our program managers Dr. Kent Miller, Dr. Kitt Reinhardt, Dr. James Hwang, and especially Dr. Gernot Pomrenke, all whom have steadfastly & patiently advised and supported our efforts throughout this award.

10. Appendices

Appendix 10.1: collected/computed data

Please see above journal publications and supporting information for collected/computed data.

Appendix 10.2: Photothermal heat transfer code written in PYTHON :

```
###############################################################################
# This script is meant to calculate internal fields and temperature profiles for an
# infinite cylinder irradiated with monochromatic light
# Author(s): Bennett Smith
# Created: 27 Jul 2015
# Updated: 29 Aug 2015

#%% Retrieve functions from external libraries
#------------------------------------------------------------------------------
from math import pi, sqrt
from scipy.special import jv, hankel1
from scipy.integrate import quad, dblquad
import scipy.optimize
import numpy as np
import matplotlib.pyplot as plt
from mpl_toolkits.mplot3d import axes3d
from matplotlib import cm

#%% Functions
#------------------------------------------------------------------------------

def d_n(r, m, n, rho1, rho2):  # Internal field coefficient from Roder et al. Langmuir, 2012
    r=1
    out = ((jv(n+1, rho2*r)*hankel1(n, rho2*r) - jv(n, rho2*r)*hankel1(n+1, rho2*r))/ \
        (((n/rho2*r) - (n*m/rho1*r))*jv(n, rho1*r)*hankel1(n, rho2*r) \
        - jv(n, rho1*r)*hankel1(n+1, rho2*r) \
        + m*(jv(n+1, rho1*r)*hankel1(n, rho2*r))))*(1/m)
    return out

def normField(r, th, rho1, rho2, jsum, ksum, e_0, m):  # Calculate internal fields
    e_1a = d_n(r, m, 0, rho1, rho2)*jv(0, rho1*r)

    e_1b = 0
    for jj in range(1, jsum):
        e_1b += ((-1)**(jj - 1))*d_n(r, m, 2*jj, rho1, rho2) * jv(2*jj, rho1*r) * np.cos(2*jj*th)

    e_1c = 0
    for kk in range(1, ksum):
        e_1c += ((-1)**(kk - 1))*d_n(r, m, 2*kk-1, rho1, rho2)*jv(2*kk-1, rho1*r)*np.cos((2*kk - 1)*th)
```

```
    field = e_0*(e_1a - 2*e_1b - 2j*e_1c)

    out = (field.real ** 2 + field.imag ** 2)/(e_0 ** 2)

    return out

#%% Infinite cylinder material properties
#--------------------------------------------------------------------------
# Expand as needed for different materials
def N_Si(wl): # Values from luxpop.com
    return {
        532 : 4.150+0.0440j,
        975 : 3.604+0.0025j,
        980 : 3.6014+0.0005763j,
        1064: 3.562+0.0010j,
    }[wl]

#%% Input
#--------------------------------------------------------------------------
diam = 550  # Cylinder diameter in nm
lambda_nm = 1064  # Laser wavelength in nm
N_1 = N_Si(lambda_nm) # Check for value from material properties
kappa_1 = 149  # W/m·K; material thermal conductivity
N_2 = 1.45 # + 0.0000000014992j  # Complex refractive index of surrounding water medium
kappa_2 = 10.0 # 0.58  # Medium thermal conductivity
eigno = 14  # Number of eigenvalues;
irrad = 1000.0  # Laser irradiance in kW/cm^2
T_inf = 298.0  # Ambient temperature (K)
Nu = 0.32 # Nusselt number; taken from literature; ref:

# The following variables will be used in external functions
jsum = 25  # Sums are used in calculation of internal electric field
ksum = 25

#%% Calculated constants
#--------------------------------------------------------------------------
radius = (diam/2)*1e-9  # Cylinder radius SI (m)
lambda_m = lambda_nm*1e-9  # Wavelength SI (m)
cvel = 299792458.0  # Velocity of light in vacuum SI (m s^-1)
epsilon_0 = 8.854188e-12  # Free Space permittivity SI (F m^-1=W s V^-2 m^-1)
mu_0 = 1.2566e-6  # Magnetic permeability SI (N A^-2)
sigma = 4*pi*N_1.real*N_1.imag/(lambda_m*mu_0*cvel)  # Optical conductivity
Biot = (kappa_2/kappa_1)*(Nu/2)

# The following constants will be used in external functions
rho1 = 2*pi*N_1*radius/lambda_m
rho2 = 2*pi*N_2*radius/lambda_m
m = N_1/N_2
```

```
E_0 = sqrt((2/(cvel*epsilon_0*N_2.real))*irrad*1.e7)  # Incident electric field
srcConstant = sigma * radius**2 * E_0**2/(2 * kappa_1 * T_inf)

#%% Source
#----------------------------------------------------------------------------
N_rth = 150
th = np.linspace(0, 2*pi, N_rth)
r = np.linspace(0, 1, N_rth)
TH, R = np.meshgrid(th, r)
X = R * np.cos(TH)
Y = R * np.sin(TH)
Xnm = X * radius * 10**9
Ynm = Y * radius * 10**9
fieldMtrx = normField(R, TH, rho1, rho2, jsum, ksum, E_0, m)

# Plot source
fig = plt.figure()
ax = fig.add_subplot(111, projection='3d')
ax.plot_surface(Xnm, Ynm, fieldMtrx, rstride=2, cstride=1, cmap=cm.coolwarm, linewidth=0)
ax.set_xlabel('\nX (nm)')
ax.set_ylabel('\nY (nm)')
ax.set_zlabel('EE*/E$_{0}$$^{2}$')
#ax.view_init(elev=90., azim=0)
plt.savefig('sourced550lamdba1064Irrad1000')

#%% Find eigenvalues
#----------------------------------------------------------------------------
step = pi / 2
a = (eigno, eigno)
Ljk = np.zeros(a)
xplot = np.linspace(0, 20, 500)
fig2 = plt.figure()
for k in range(eigno):
    count = 0
    test = 0.05 #0.1
    if k > 1:
        test = Ljk[0, k - 1] + step
    def FL(x):
        if k == 0:
            return - x * jv(k + 1, x) + Biot * jv(k, x) # From Langmuir Paper
        else:
            return (k/x) * jv(k, x) - jv(k + 1, x) + Biot * jv(k, x) # From Langmuir Paper
    yplot = FL(xplot)
    if k >= 0:
        plt.plot(xplot, yplot) # Plot eigenvalue functions
    while Ljk[eigno - 1, k] == 0: # Find roots until Ljk is filled
        xcheck = scipy.optimize.fsolve(FL, test)
        if Ljk[0, k] == 0 and xcheck > 0.001: # Assign Initial Eigenvalue; minumum set to .001
            if xcheck > k * 4 and k > 0:
```

```
            test = xcheck - 3 * step
        else:
            Ljk[count, k] = xcheck
            count = count + 1
    elif Ljk[0, k] != 0 and xcheck > Ljk[count - 1, k] + 6: # Check for overshoot for subsequent
eigenvalue
        test = xcheck - 3 * step
    elif Ljk[0, k] != 0 and xcheck > Ljk[count - 1, k] + 1: # Check for repeated eigenvalue and assign
        Ljk[count, k] = xcheck
        count = count + 1
    test = test + step
#plt.savefig('EigenvalueFxns')

#%% Calculate Norms
#------------------------------------------------------------------------------
Njk = np.zeros(a)
for j in range(eigno):
  for k in range(eigno):
    def FN(x):
      return x * jv(k, Ljk[j,k] * x) * jv(k, Ljk[j,k] * x)
    Njk[j, k] = quad(FN, 0, 1)[0]

#%% Build constant matrix
#------------------------------------------------------------------------------
Bjk = 1 / (Ljk**2 * Njk)

#%% Calculate Ajk coefficient
#------------------------------------------------------------------------------
def FA(x,t):
  return (2 / pi) * Bjk[j, k] * x * jv(k, Ljk[j, k] * x) \
    * np.cos(k * t) * normField(x, t, rho1, rho2, jsum, ksum, E_0, m)

Ajk = np.zeros(a)
for j in range(eigno):
  for k in range(eigno):
    Afxn = srcConstant * FA(R,TH)
    I = np.zeros(N_rth)
    for i in range(N_rth):
      I[i] = np.trapz(Afxn[i,:], r) # Trapezoidal method solves in reasonable amount of time
    Ajk[j, k] = np.trapz(I, th)

# Unable to get dblquad to solve in reasonable time lengths, even though matlab does
#for j in range(eigno):
#  for k in range(eigno):
#    Ajk[j, k] = srcConstant * dblquad(FA, 0, 1, lambda x: 0, lambda x: pi)[0]
#    print(Ajk[j,k])

#%% Calculate temperature
#------------------------------------------------------------------------------
```

```
phi = np.zeros((N_rth, N_rth))
for j in range(eigno):
    for k in range(eigno):
        phi += (2 / pi) * Ajk[j, k] * jv(k, Ljk[j, k] * R) * np.cos(k * TH)

tempK = phi * T_inf + T_inf
tempC = tempK-273

fig3 = plt.figure()
ax = fig3.add_subplot(111, projection='3d')
ax.plot_surface(Xnm, Ynm, tempC, rstride=2, cstride=1, cmap=cm.coolwarm, linewidth=0)
ax.set_xlabel('\nX (nm)')
ax.set_ylabel('\nY (nm)')
ax.zaxis.set_major_formatter(plt.FormatStrFormatter('%.3f'))
ax.set_zlabel('\n\n' + 'Temperature (C)', linespacing = 1.8)
ax.tick_params(axis='z',pad=10)
plt.savefig('temperatured550lamdba1064Irrad1000')
```

Appendix 10.3: Description of the experimental equipment, set up, and procedures:

A single-beam laser trapping apparatus was assembled using a laser wavelength of 1020 nm. A home-built laser trapping instrument was used to observe the Brownian dynamics of individual Yb3+:YLF nanocrystals. Briefly, the single-beam laser trap was used to extract the surrounding local temperature profile of YLF particles through observations of forward-scattered laser radiation profiles that are processed to yield both the calibrated power spectral density and diffusion coefficient for individual YLF crystals. The laser refrigeration of 10% (mol%) Yb3+:YLF (i.e., 10% Yb3+ ions, 90% Y3+ ions) nanocrystals by more than 10 °C in PBS and Dulbecco's modified Eagle medium (DMEM) was observed at a trapping wavelength of λ = 1,020 nm.

The laser tweezer setup is a modified modular optical tweezer kit (Thorlabs, OTKB), where the original condenser lens has been replaced with a 10× Mitutoyo condenser (Plan Apo infinity-corrected long WD objective, stock no. 46–144). The 100× objective focusing lens has a numerical aperture of 1.25 and a focal spot of 1.1 μm. The quadrant photodiode (QPD) and piezostage were interfaced to the computer through a DAQ card (PCIe-6361 X series, National Instruments) and controlled through modified MATLAB software (Thorlabs). Experimental chambers were prepared as follows. Several

microliters of the nanocrystal/aqueous medium dispersion were transferred by a pipette into a chamber consisting of a glass slide and glass coverslip. The edges of the glass slide and the glass coverslip were then sealed with a 150-μm-thick adhesive spacer (SecureSeal Imaging Spacer, Grace Bio-laboratories). Nanocrystals were trapped at the center (~75 μm from the surface) of the temperature-controlled perfusion chamber (RC-31, Warner Instruments) and held at T0 = 25 °C while voltage traces were recorded at the QPD for 3 s at a sample rate of 100 kHz. The QPD voltage signal was calibrated by oscillating the piezostage at 32 Hz and an amplitude of 150 nm peak-topeak during signal acquisition. Trapping data were acquired using a diode-pumped solid-state Yb3+:YAG thin-disk tunable laser (VersaDisk 1030–10, Sahajanand Laser Technologies) at a wavelength of 1,020 nm, a 975-nm pigtailed fiber Bragg grating stabilized single-mode laser diode (PL980P330J, Thorlabs), as well as a solid-state Nd3+:YAG 1,064-nm (BL-106C, Spectra-Physics) at an irradiance of 5.9, 10.7, 14.6, 21.2, and 25.5MW/cm2. Each YLF cooling data point collected represents an average of six individual particles with an average radius of 764 nm with an SD of 293 nm. Silica beads (SS04N/9857, Bangs Laboratories) were used for their monodisperse size distribution (1,010-nm diameter), and they have shown to minimally heat when trapped with a laser tweezer at NIR wavelengths. Electromagnetic simulations of the interaction of the trapping laser with an YLF TTB were also performed using the discrete dipole approximation (DDSCAT) to predict the stable trapping configurations of optically trapped YLF particles. Lastly, visible emission of Er3+ from Er/Yb codoped trapped YLF host crystals was detected using an Acton SpectraPro 500i spectrograph with a Princeton liquid-nitrogen-cooled Si detector.

Power spectra from the QPD voltage traces were processed according to Berg-Sorensen and Flyvbjerg and used to calibrate the QPD traces following the method of Tolic-Norrelykke. An experimental diffusion coefficient was then extracted by fitting the characteristic function for the experimental power spectra derived in Berg-Sorensen and Flyvbjerg. Given that the temperature of the trapped particle is significantly different from the temperature sufficiently far from the laser focus, the

particle–trap system is not isothermal and behaves according to nonequilibrium dynamics. Thus, equating the experimental diffusion coefficient to nonisothermal Brownian dynamics necessitates the application of CBM, as derived by Chakraborty et al..

AFOSR Deliverables Submission Survey

Response ID:9245 Data

1.

Report Type

Final Report

Primary Contact Email

Contact email if there is a problem with the report.

bethz2@uw.edu

Primary Contact Phone Number

Contact phone number if there is a problem with the report

206-543-3538

Organization / Institution name

University of Washington

Grant/Contract Title

The full title of the funded effort.

Laser Refrigeration of Optically-Insulated Cryophotonic Nanocrystals

Grant/Contract Number

AFOSR assigned control number. It must begin with "FA9550" or "F49620" or "FA2386".

FA9550-12-1-0400

Principal Investigator Name

The full name of the principal investigator on the grant or contract.

Dr. Peter Pauzauskie

Program Officer

The AFOSR Program Officer currently assigned to the award

Dr. Gernot Pomrenke

Reporting Period Start Date

04/16/2012

Reporting Period End Date

12/29/2015

Abstract

The demonstration of anti-Stokes laser refrigeration to cryogenic temperatures with macroscopic YLF crystals doped with Yb3+ rare-earth ions has resulted in a new approach for solid state laser refrigeration. There are remarkable changes in a material's density of states (electron, phonon, or photon), optical absorption, radiative lifetime, thermal conductivity, and light scattering properties when the material's size is reduced below optical wavelengths. One outstanding question in the field is the extent to which a nanoscale YLF crystal's size and morphology will enhance its external radiative quantum efficiency and subsequent performance in solid state laser refrigeration.

Distribution Statement

This is block 12 on the SF298 form.

Distribution A - Approved for Public Release

Explanation for Distribution Statement

If this is not approved for public release, please provide a short explanation. E.g., contains proprietary information.

SF298 Form

Please attach your SF298 form. A blank SF298 can be found here. Please do not password protect or secure the PDF The maximum file size for an SF298 is 50MB.

PP_SF298_FA9550-12-1-0400-1.pdf

Upload the Report Document. File must be a PDF. Please do not password protect or secure the PDF . The maximum file size for the Report Document is 50MB.

FA9550-12-1-0400_final_report.pdf

Upload a Report Document, if any. The maximum file size for the Report Document is 50MB.

Archival Publications (published) during reporting period:

New discoveries, inventions, or patent disclosures:
Do you have any discoveries, inventions, or patent disclosures to report for this period?

Yes

Please describe and include any notable dates

1. Title: "Laser refrigeration of inorganic nanocrystals in liquid water"
Inventors: Peter Pauzauskie; Paden Roder; Bennett Smith; Xuezhe Zhou
UW Ref. 46874, disclosed on 3/11/2014
Patent application: 15/351,352, filed on 11/14/2016

2. Title: "Morphology dependent energy transfer in semiconductor nanowires"
Inventors: Peter Pauzauskie; James Davis; Paden Roger; Bennet Smith
UW Ref. 46304, disclosed on 11/2/2012
Patent application: none

3. Title: "Photothermal Superheating of Water with Ion-implanted Silicon Nanowires"
Inventors: Peter Pauzauskie; Paden Roder; Bennet Smith; Xuezhe Zhou
UW Ref. 47398, disclosed on 7/9/2015
Patent application: PCT/US2016/042857, filed on 7/18/2016

Do you plan to pursue a claim for personal or organizational intellectual property?

Yes

Changes in research objectives (if any):

Change in AFOSR Program Officer, if any:

Extensions granted or milestones slipped, if any:

AFOSR LRIR Number

LRIR Title

Reporting Period

Laboratory Task Manager

Program Officer

Research Objectives

Technical Summary

Funding Summary by Cost Category (by FY, $K)

	Starting FY	FY+1	FY+2
Salary			
Equipment/Facilities			
Supplies			
Total			

Report Document

Report Document - Text Analysis

Report Document - Text Analysis

Appendix Documents

2. Thank You

E-mail user

Jan 09, 2018 15:35:51 Success: Email Sent to: bethz2@uw.edu